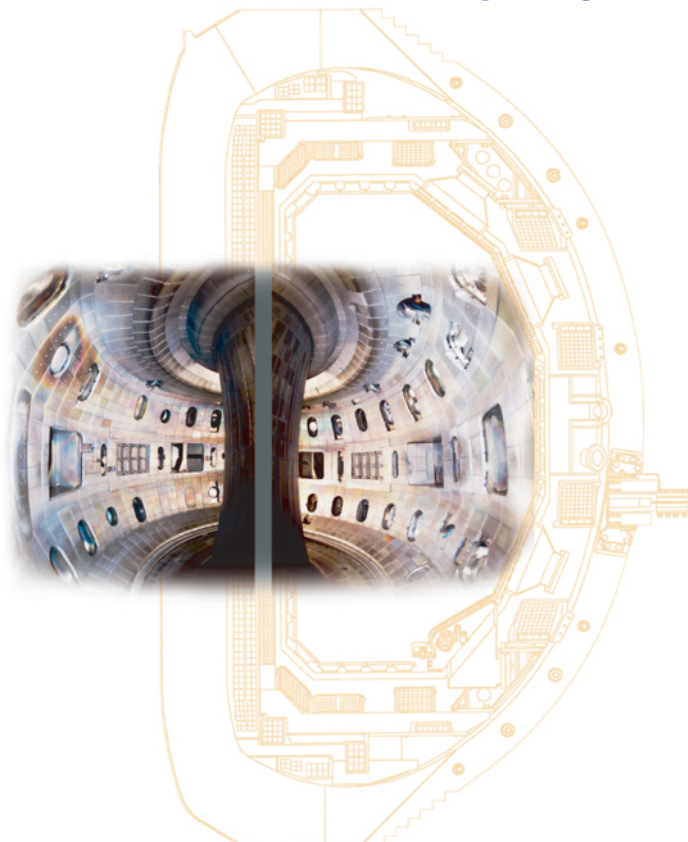


# Implications of Wall Recycling and Carbon Source Locations on Core Plasma Fueling and Impurity Content in DIII-D



<sup>1</sup>M. Groth and <sup>1</sup>G.D. Porter

<sup>2</sup>J.A. Boedo, <sup>3</sup>N.H. Brooks, <sup>1</sup>M.E. Fenstermacher,

<sup>3</sup>R.J. Groebner, <sup>1</sup>C.J. Lasnier, <sup>1</sup>W.H. Meyer,

<sup>2</sup>R.A. Moyer, <sup>4</sup>L.W. Owen, <sup>3</sup>T.W. Petrie,

<sup>1</sup>M.E. Rensink, <sup>4</sup>D.L. Rudakov, <sup>5</sup>G. Wang, <sup>6</sup>J.G. Watkins,

<sup>1</sup>N.S. Wolf, <sup>5</sup>L.Zeng

<sup>1</sup>Lawrence Livermore National Laboratory, CA, USA

<sup>2</sup>University of California, San Diego CA, USA

<sup>3</sup>General Atomics, San Diego, CA, USA

<sup>4</sup>Oak Ridge National Laboratory, TN, USA

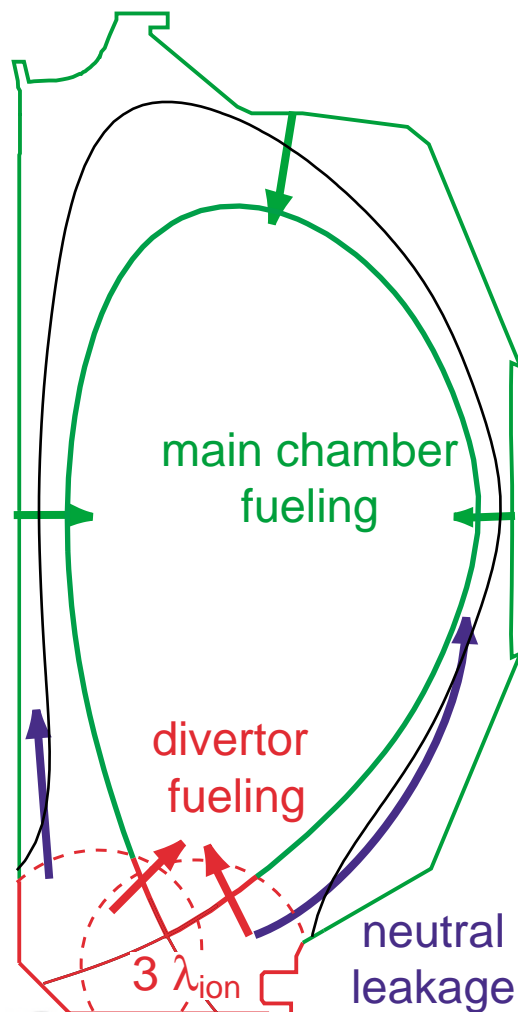
<sup>5</sup>University of Los Angeles, CA, USA

<sup>6</sup>Sandia National Laboratory, NM, USA

The 20th IAEA Conference Fusion Energy Conference  
Vilamoura, Portugal

November 1–6, 2004

# Motivation: Poloidal distribution of core plasma fueling and impurity sources affect core plasma performance



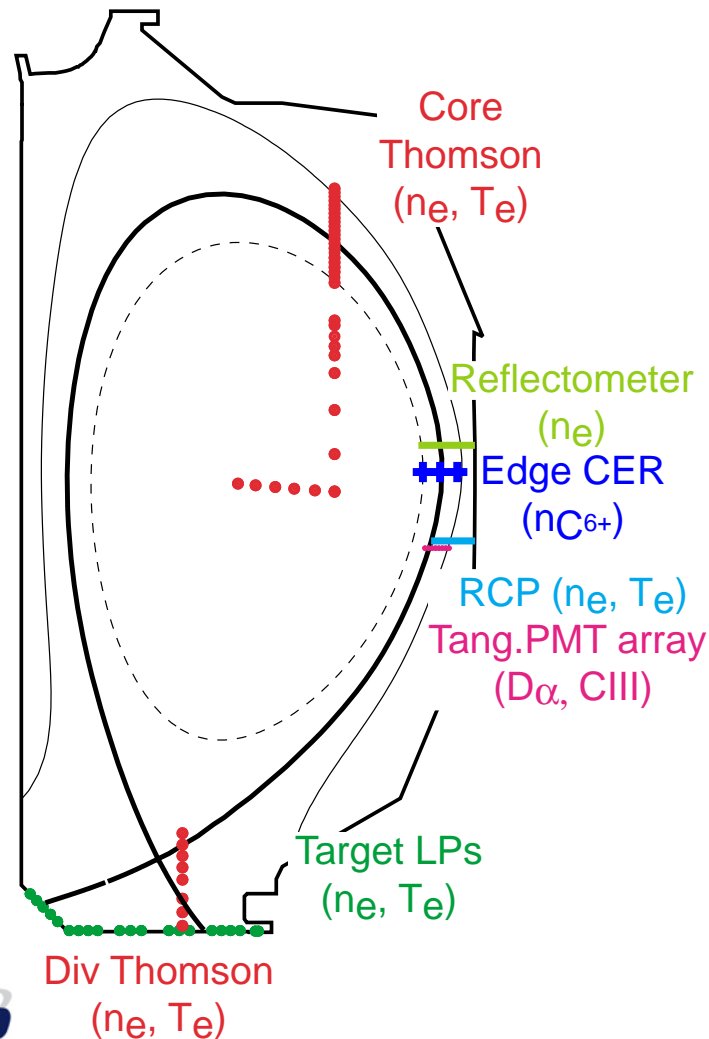
- Fuel source distribution modifies height and width of H-mode density pedestal [*Mahdavi et al. PoP 2003*]
- Core power balance is sensitive to impurity content
  - Understanding needed to predict performance in future devices
- Three principal fueling channels:
  - Div. → x-point region → core
  - Div. → neutral leakage → core
  - Main walls → core
- More efficient screening of divertor sources due to divertor geometry than main wall sources

# Summary and methodology

---

- Poloidal distribution of fueling in L-mode and ELMy H-mode suggests that ...
  - Dominant core plasma fueling occurs near divertor X-point region due to recycling at the divertor targets
  - Significant neutral leakage from divertor into inner main SOL
  - Divertor target plates and divertor walls are dominant carbon sources
  - Carbon ion leakage from divertor into main SOL is the main transport mechanism that sets core carbon content
- Methodology
  - Detailed measurement of plasma parameters in main and divertor SOL, including 2-D emission distribution of  $D_\alpha$ , CII, CIII
  - + Data-constrained UEDGE/DEGAS2 2-D boundary modeling of deuterium neutrals and ions, and carbon transport

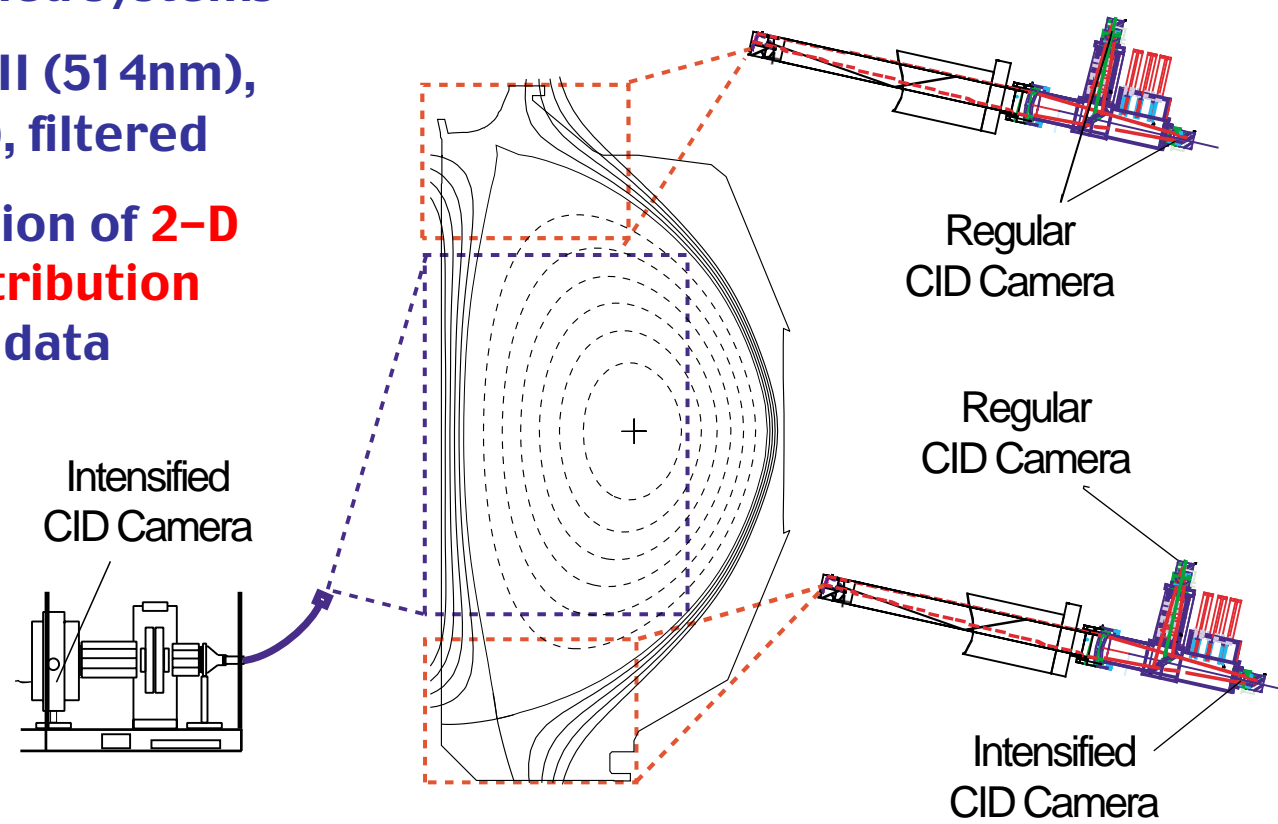
# Extensive edge diagnostic system was employed to characterize divertor and main SOL



- Spatially resolved ( $\Delta R_{mid} < 1 \text{ cm}$ ) measurement of main SOL plasma parameter in outer main SOL
  - Thomson scattering
  - Reflectometer
  - Reciprocating probe
  - Edge charge-exchange
  - Tangential PMT array
- Divertor heat and particle flux profiles
  - Target Langmuir probes
  - Infra-red camera
- 2-D n<sub>e</sub> and T<sub>e</sub> distribution in outer divertor leg using Thomson scattering

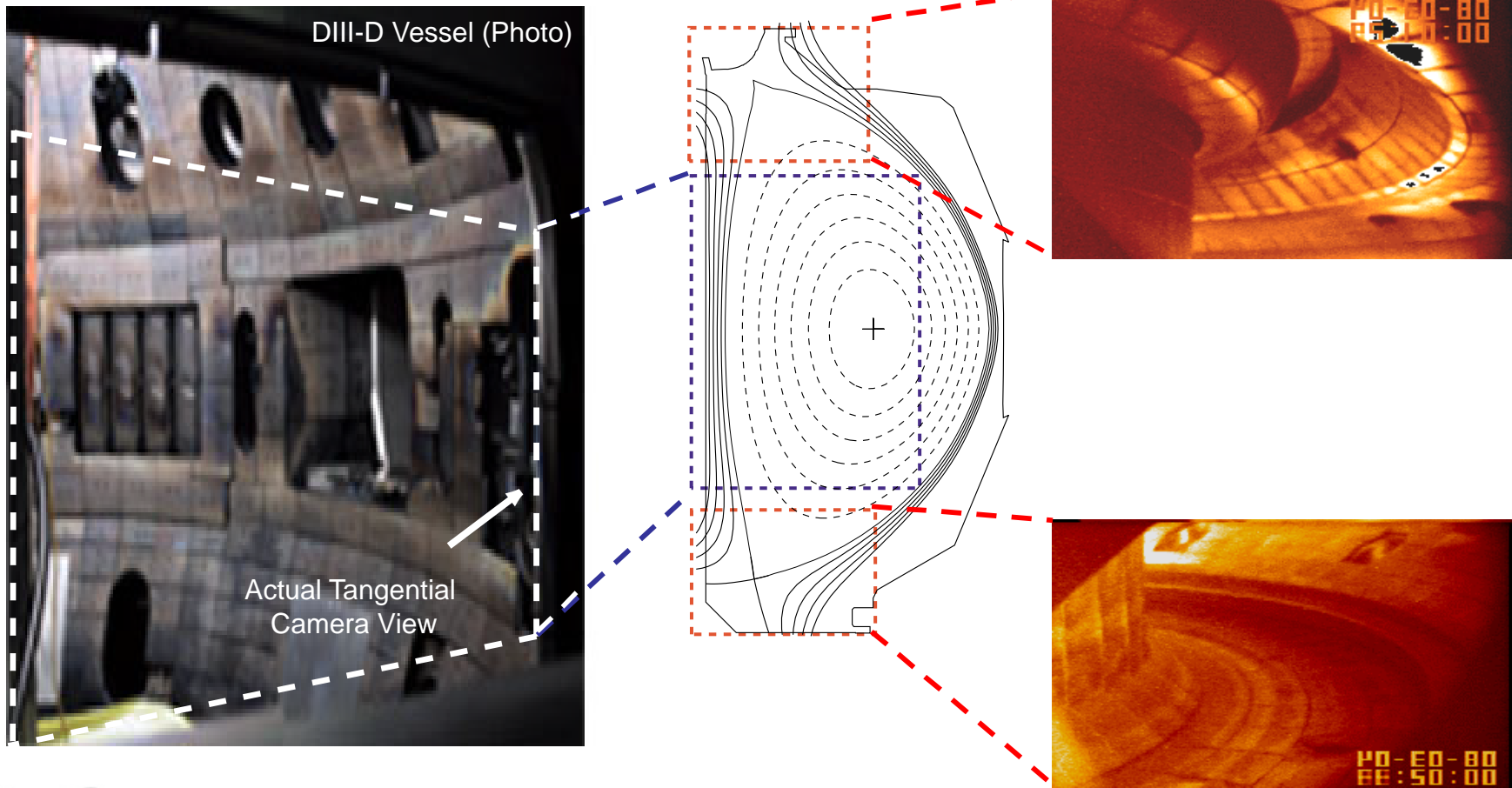
# Tangentially viewing cameras measured emission over a region of 85% of the poloidal cross-section

- Rad-hardened, 8bit CID<sup>s</sup>
- Two intensified systems
- Visible: D <sub>$\alpha$</sub> , CII (514nm), CIII (465nm), filtered
- Reconstruction of **2-D poloidal distribution** from image data

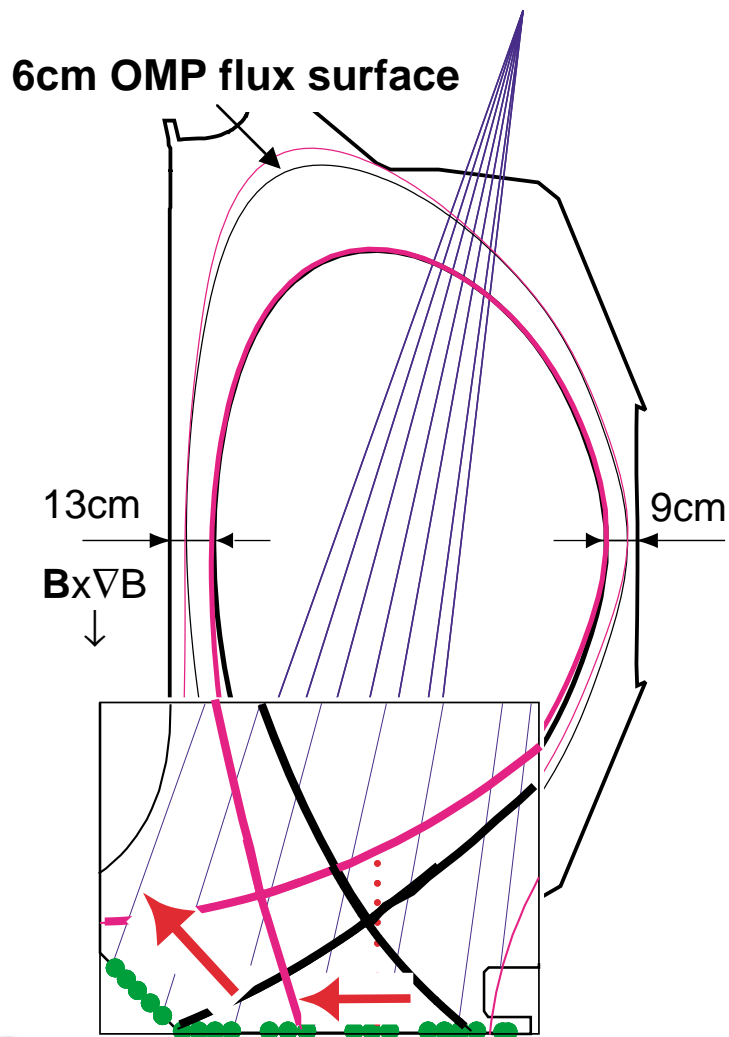


# Divertor cameras span region from target plates to 60–80cm into main chamber, midplane camera spans inner and outer SOL ( $-70\text{cm} < Z < 60\text{cm}$ )

---

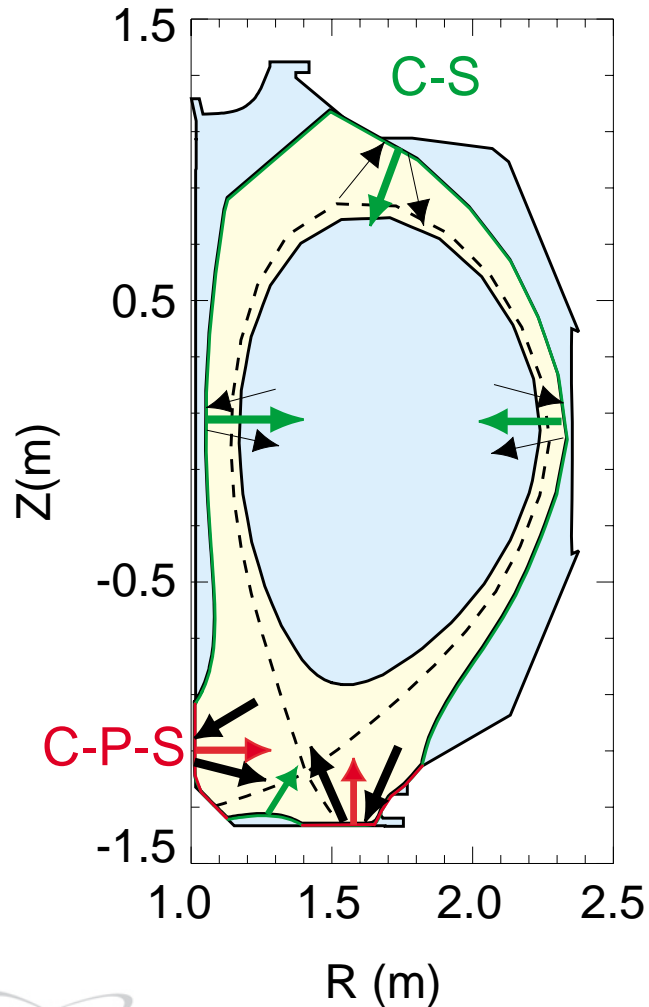


# Lower-single null L-mode with $n/n_{GW} = 0.2 \rightarrow 0.4$ optimized for diagnosis of divertor and main SOL



- Magnetic configuration
  - LSN,  $B_x \nabla B$  into lower divertor
  - Inner gap 13cm, outer gap 9cm
  - 7cm flux surface intersects upper baffle limiter
  - 30cm strike point sweep for high spatial resolution
- Three density levels, varied shot-to-shot:
  - $\langle n_e \rangle = 2.6 \times 10^{19} \text{ m}^{-3}$  ( $n/n_{GW} = 0.24$ )
  - $\langle n_e \rangle = 3.1 \times 10^{19} \text{ m}^{-3}$  ( $n/n_{GW} = 0.29$ )
  - $\langle n_e \rangle = 4.1 \times 10^{19} \text{ m}^{-3}$  ( $n/n_{GW} = 0.37$ )

# Model neutral transport with DEGAS2 on background plasma calculated by fluid edge code UEDGE

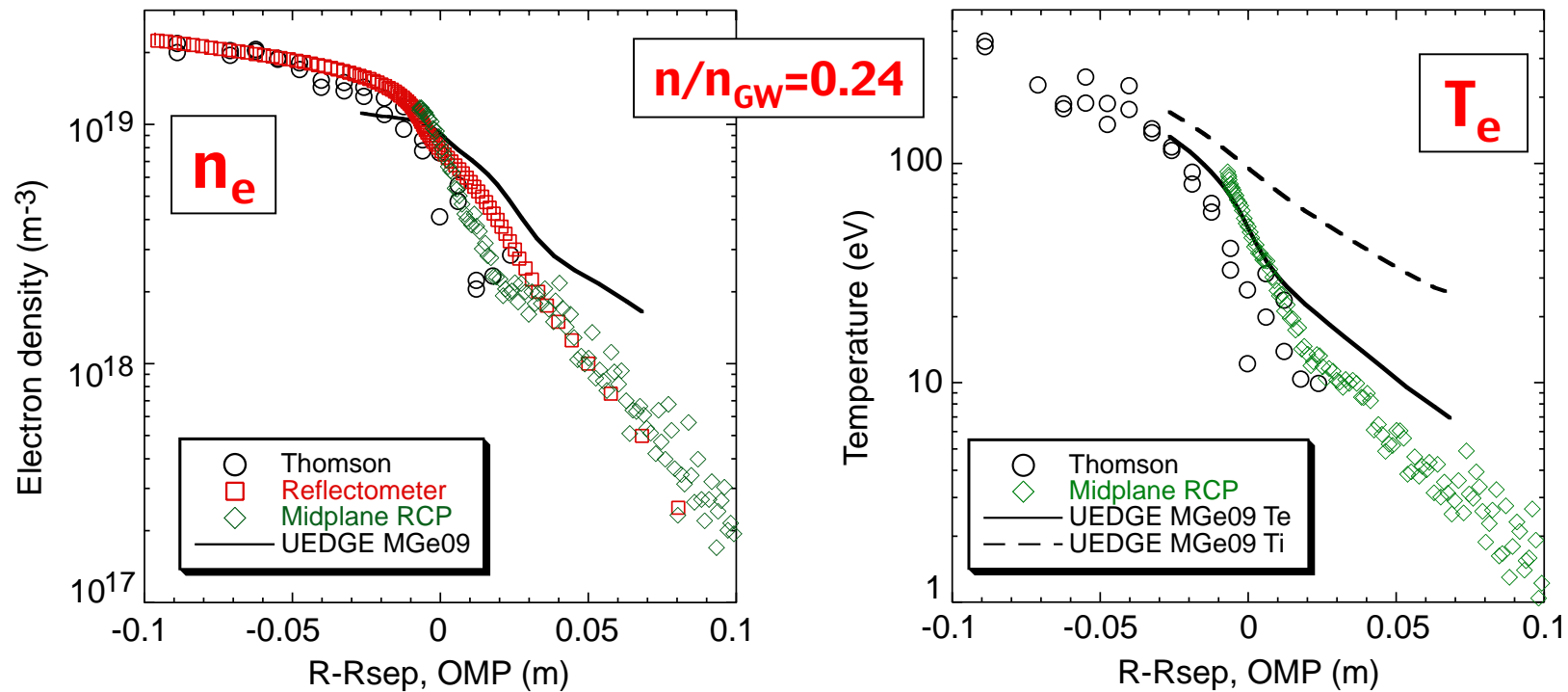


- UEDGE w/ classical drifts and carbon transport model,  $0.94 \leq \Psi_N \leq 1.15$
- Purely diffusive radial transport,  $D_{\perp}$ ,  $\chi_e, \chi_i$  spatially constant
- BC: finite ion flux across outer grid, returned as neutrals
- BC: 5% wall pumping of neutrals outer UEDGE grid boundary 20cm above targets
- Carbon: C-P-S at target, C-S at outer UEDGE grid boundary  
*[Eckstein JNM 1997, Davis JNM 1997]*
- Launch DEGAS2 neutrals from target plate, CX-walk and reflections, plasma prescription for halo region

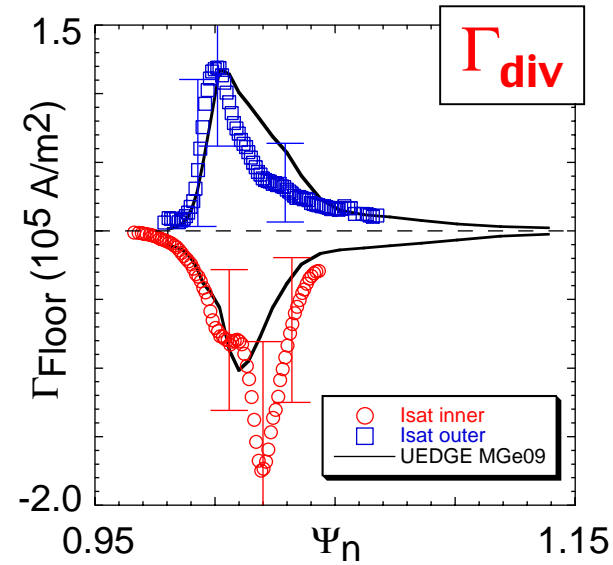
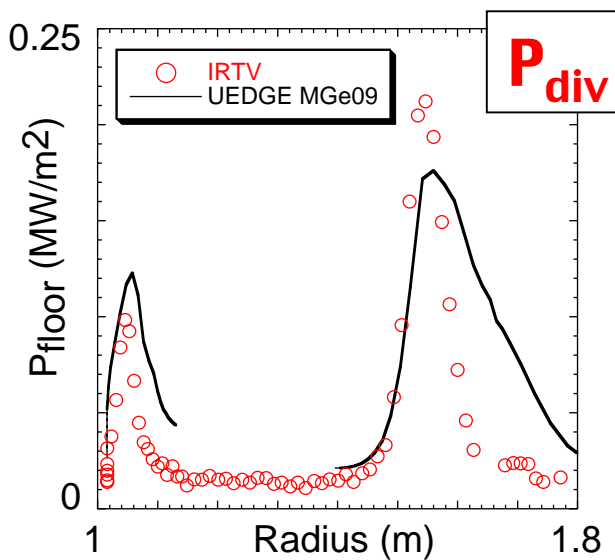
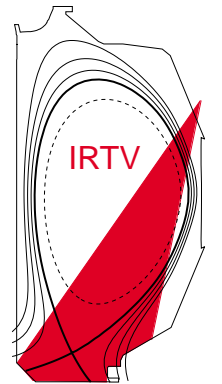
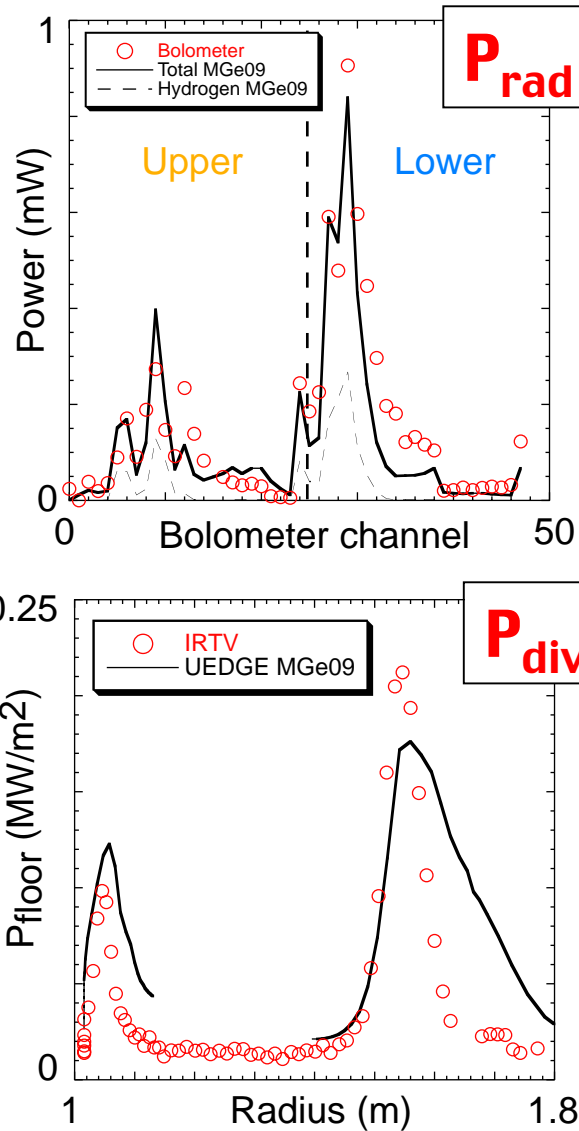
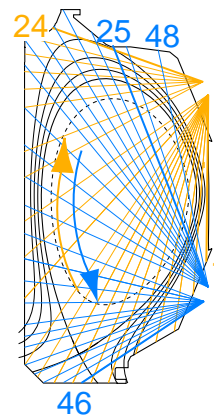
**Modeling lowest density case: Experimental core and outer main SOL  $n_e$  and  $T_e$  were simulated in UEGDE using spatially const.  $D_{\perp} = 0.65 \text{ m}^2/\text{s}$  and  $\chi_e = \chi_i = 2.6 \text{ m}^2/\text{s}$**

---

- Excellent agreement in experimental upstream  $n_e$  and  $T_e$  parameters measured by three independent techniques



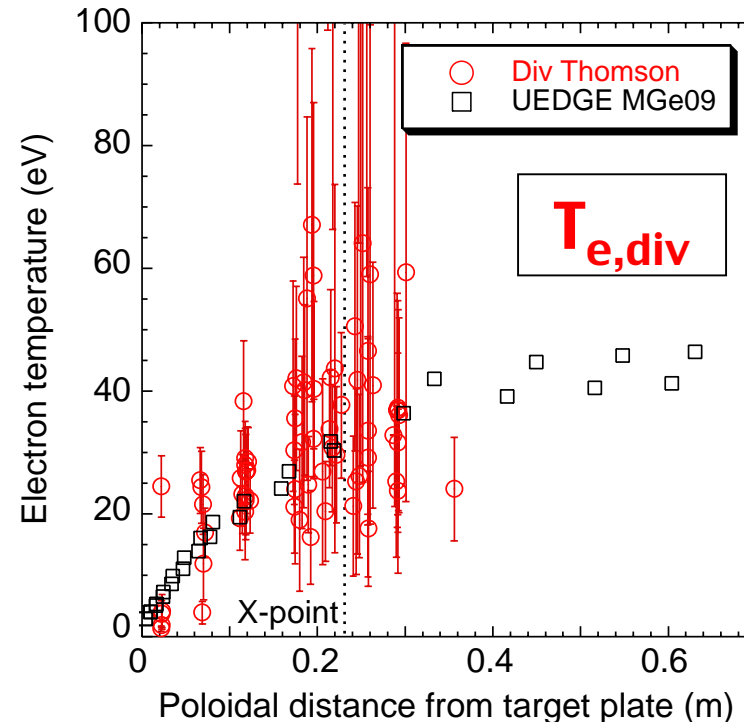
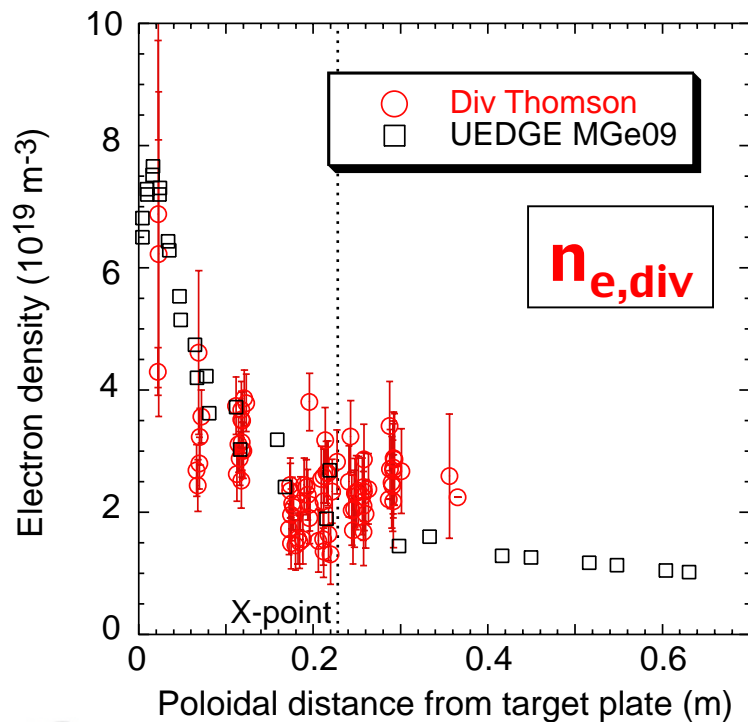
# UEDGE simulation match experimental total radiated power, divertor heat flux, and particle flux to divertor plates to within factor of 2



- LP analysis:
  - $T_{e, \text{OSP}} \approx 25\text{eV} \rightarrow \text{well-attached outer leg}$
  - $T_{e, \text{ISP}} \leq 8\text{eV} \rightarrow \text{partially detached inner leg}$

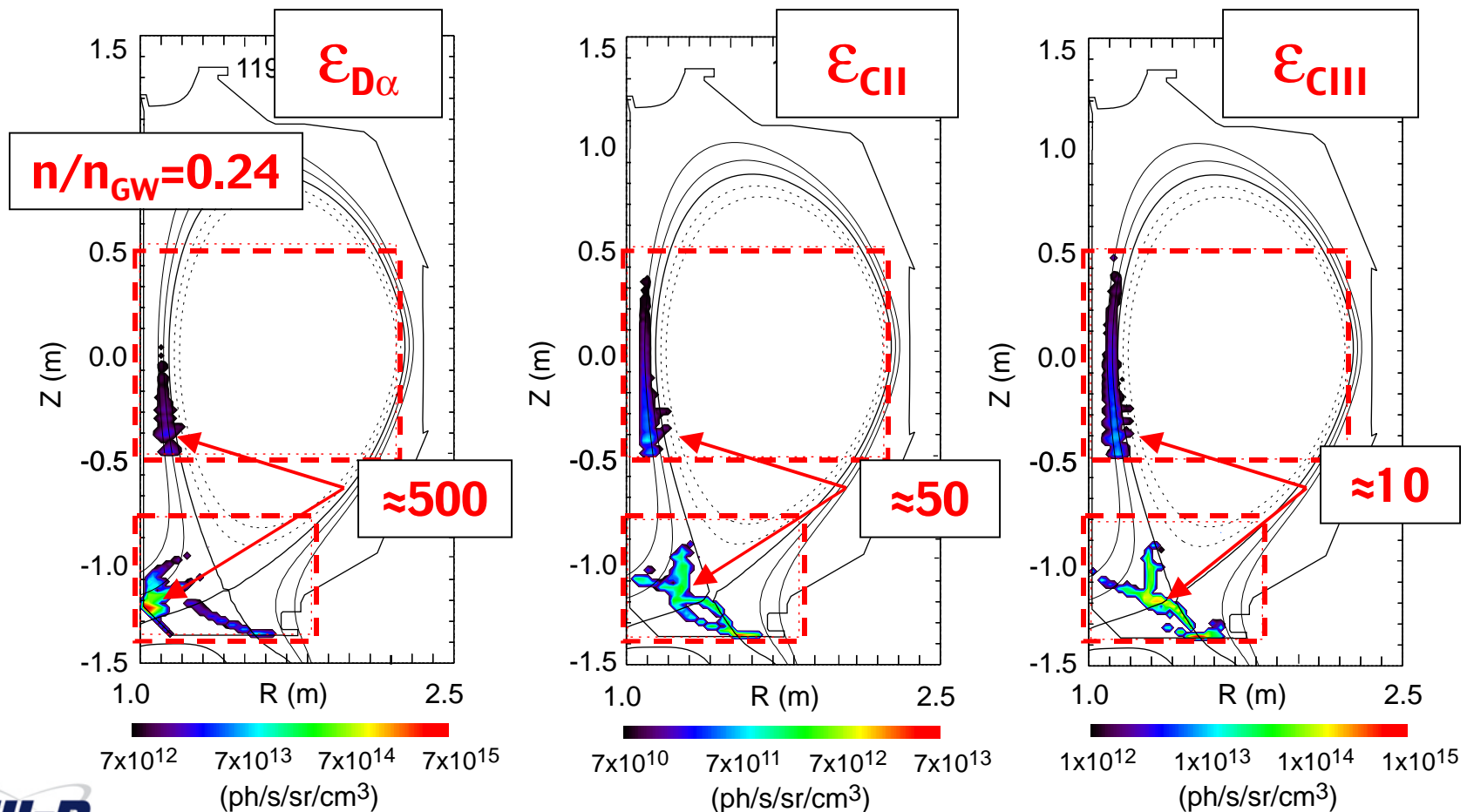
# UEDGE simulation also agree with divertor Thomson $n_e$ and $T_e$ profiles in outer divertor leg

- Near-separatrix divertor Thomson data in common SOL obtained during strike point sweep:  $1.002 \leq \Psi_N \leq 1.008$
- $T_e$  just above target plate unusually low – known problem with Thomson analysis, UEDGE calculated  $T_e$  at plate  $\rightarrow 2\text{eV}$

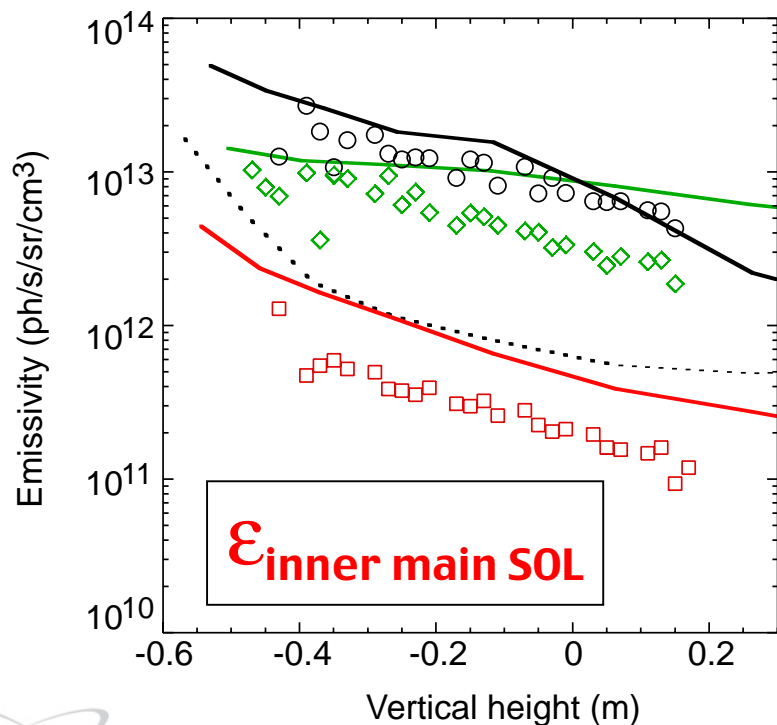
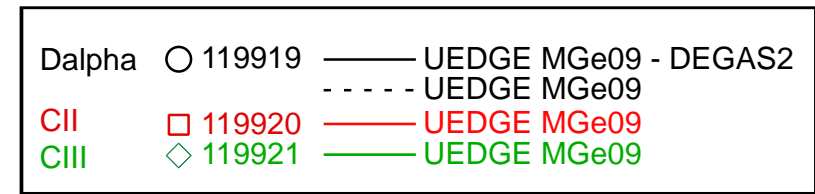


# Experimental 2-D intensity distribution of $D_{\alpha}$ , CII, and CIII is dominated by emission from the divertor

- CII and CIII emission well off inner divertor target plates  
→ Te of inner divertor plasma < 5eV, consistent w/ LP measurements



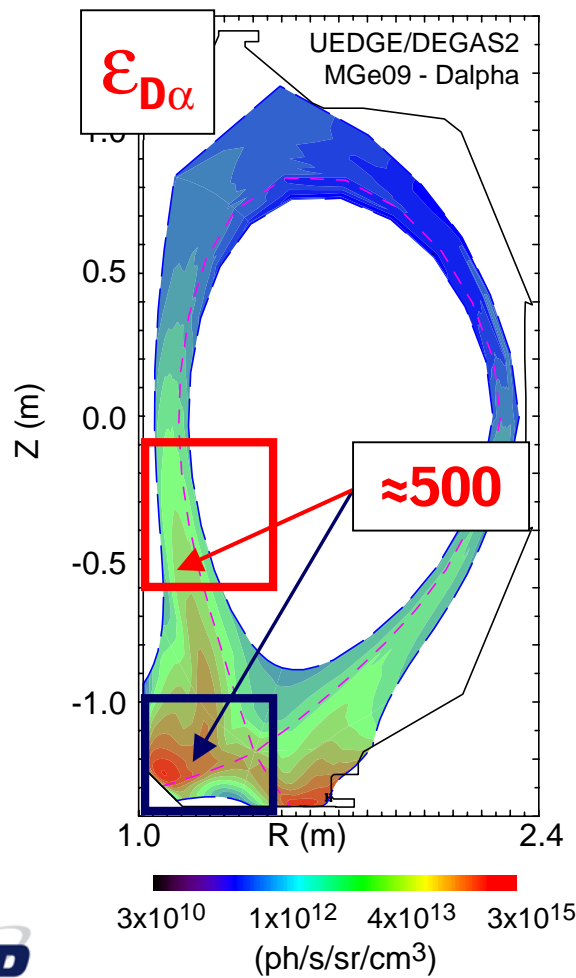
# Inner midplane emission D <sub>$\alpha$</sub> , CII, and CIII peaks in region nearest to divertor X-point



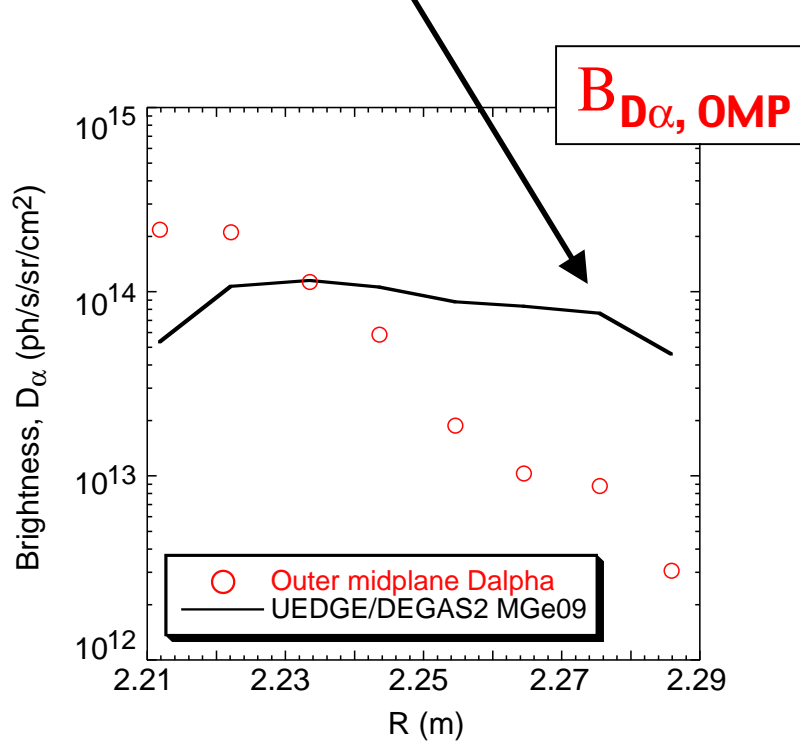
|  |      |      |      |
|--|------|------|------|
| $\langle n_e \rangle (10^{19} \text{ m}^{-3})$ | 2.6  | 3.1  | 4.1  |
| $n/n_{GW}$                                     | 0.24 | 0.29 | 0.37 |
| $L_{\text{pol},D\alpha} (\text{m})$            | 0.5  | 0.4  | 0.4  |
| $L_{\text{pol},\text{CII}} (\text{m})$         | 0.3  | 0.4  | 0.3  |
| $L_{\text{pol}, \text{CIII}} (\text{m})$       | 0.3  | 0.3  | 0.5  |

- Poloidal fall-off length in inner midplane SOL  $\sim 0.3\text{m} - 0.5\text{m}$
- Poloidal variation of inner midplane emission only weakly sensitive to core (and divertor) densities

# Calculated $D_\alpha$ emission using UEDGE/DEGAS2 agrees quantitatively with measurements in lower divertor and inner midplane region

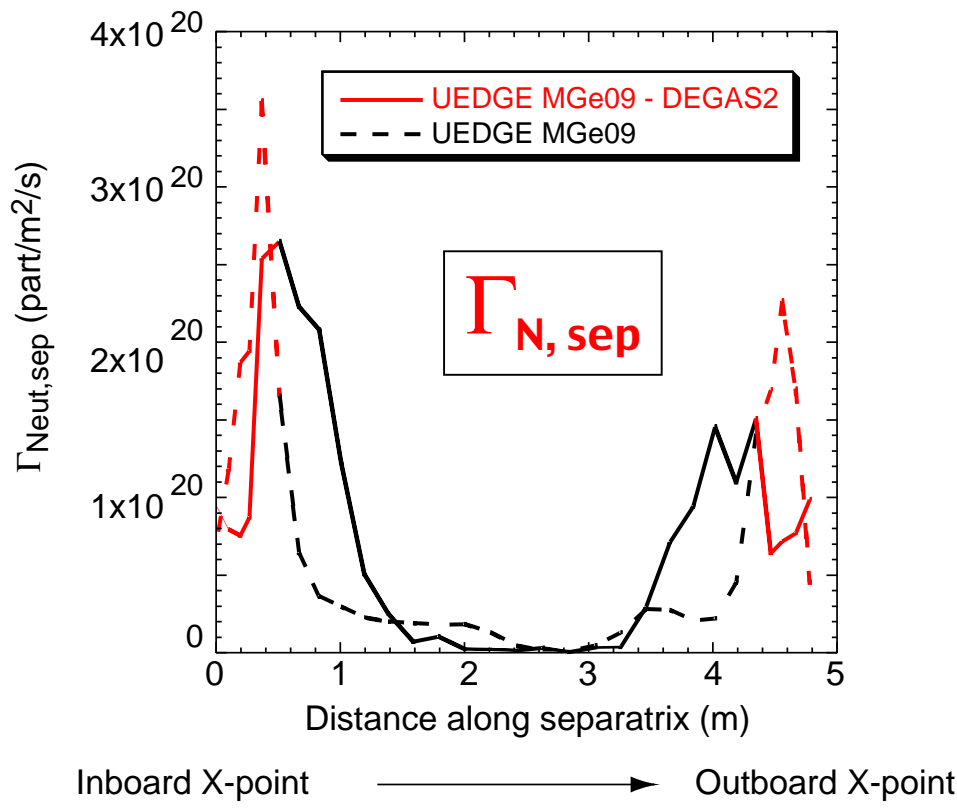


- Order-of-magnitude  $D_\alpha$  emissivity matched, but far-SOL  $D_\alpha$  overestimated by UEDGE/DEGAS2



# UEDGE/DEGAS2 simulations indicate that core plasma is fueled by divertor X-point region and neutral leakage

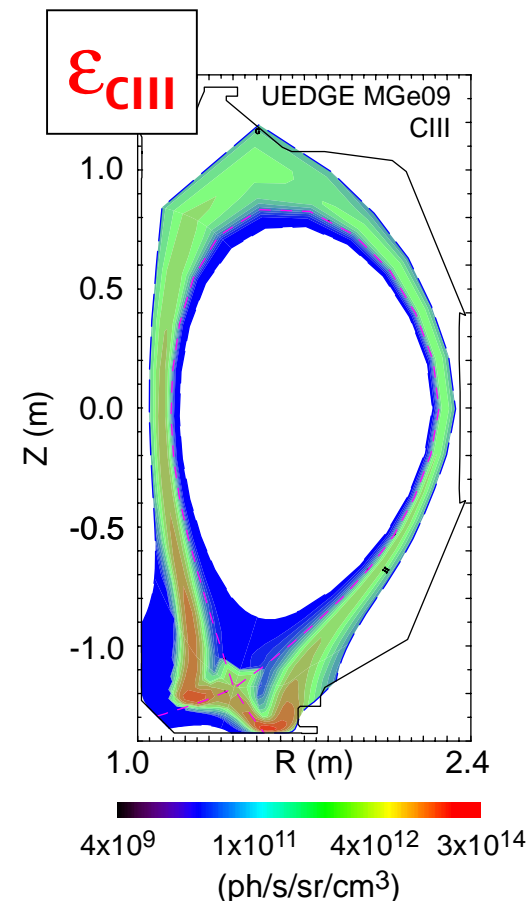
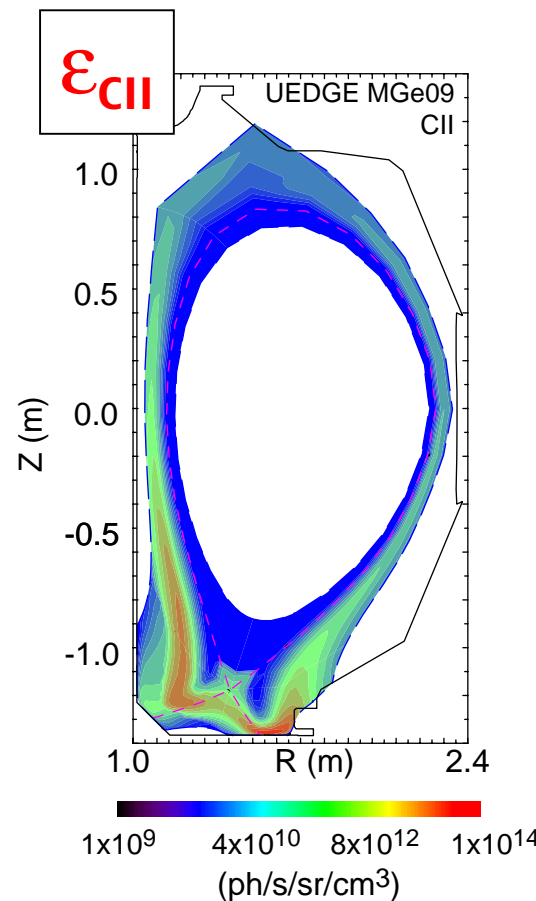
---



- **DEGAS2: Comparable fueling through X-point region and due to neutral leakage (42% divertor vs. 58% leakage)**
  - **UEDGE alone (w/o neutral leakage in halo region): stronger X-point fueling (71% div. vs. 29% leakage)**
- **Poloidal core fueling profile sensitive to whether and how halo plasma region is modeled**

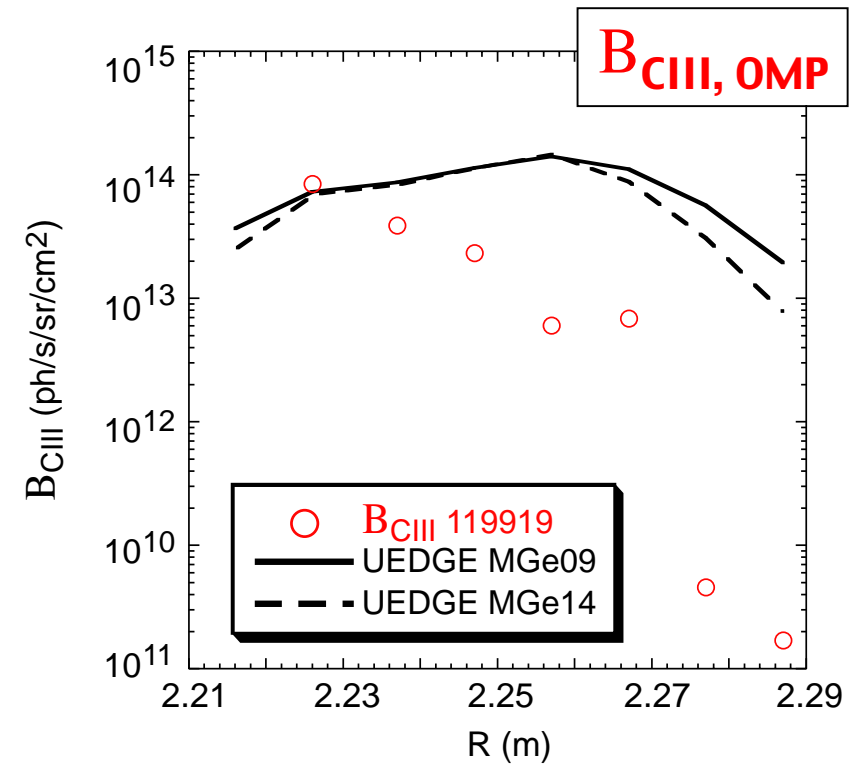
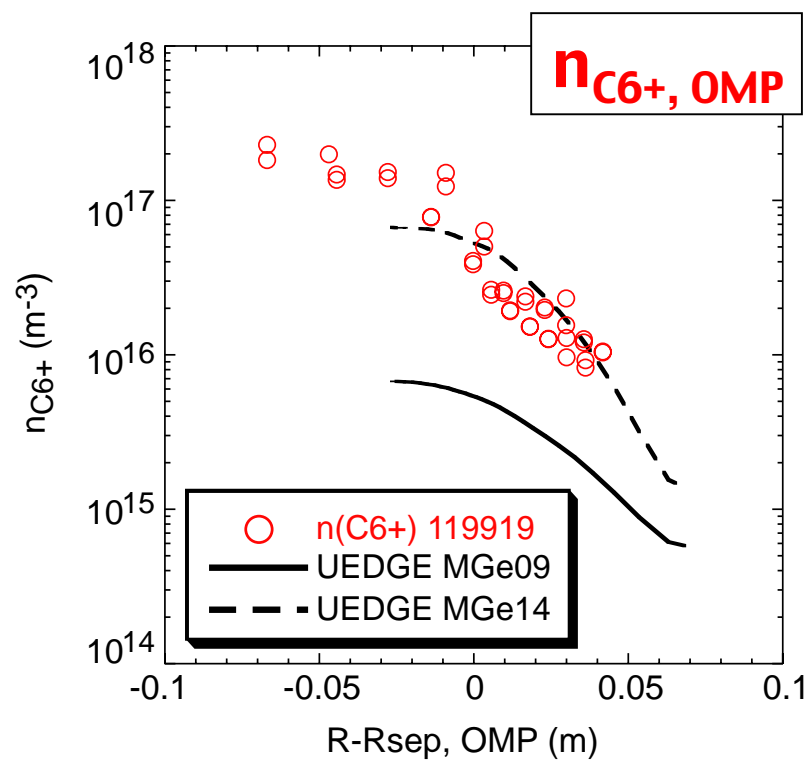
# UEDGE-simulated CII and CIII distribution peaks well above inner divertor target plate → due to significantly colder inner divertor plasma than outer

- Higher fraction of low-charge-state carbon in inner main SOL than in outer, poloidally extended toward plasma “top”



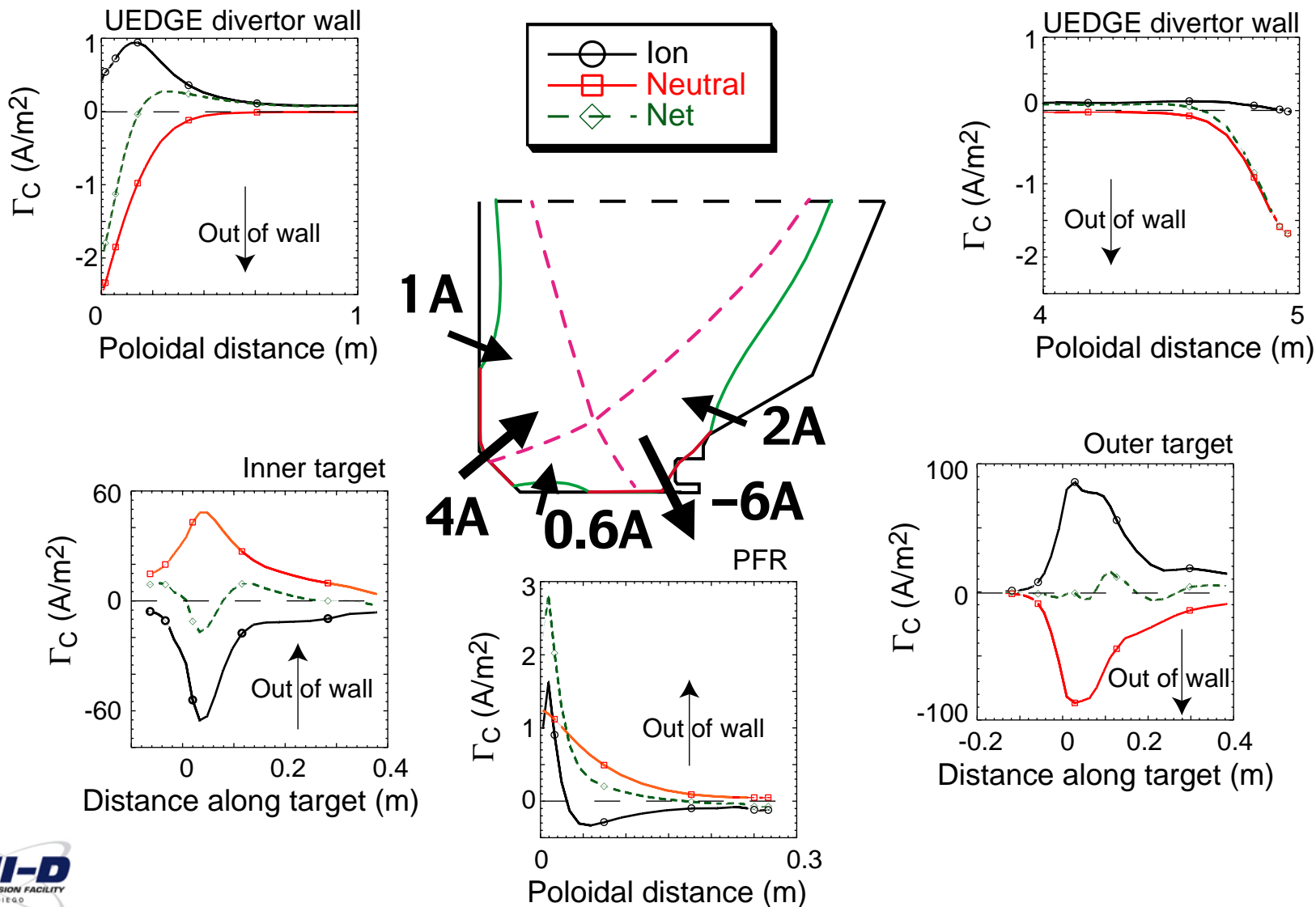
# Small changes of diffusivities for carbon has strong effect on high-charge state density profiles

- Decreasing all (particle and heat) diffusivities by 35% changes  $n_{C6+}$  by an order of magnitude (!)
- Low-charge-state carbon emission more robust to these changes

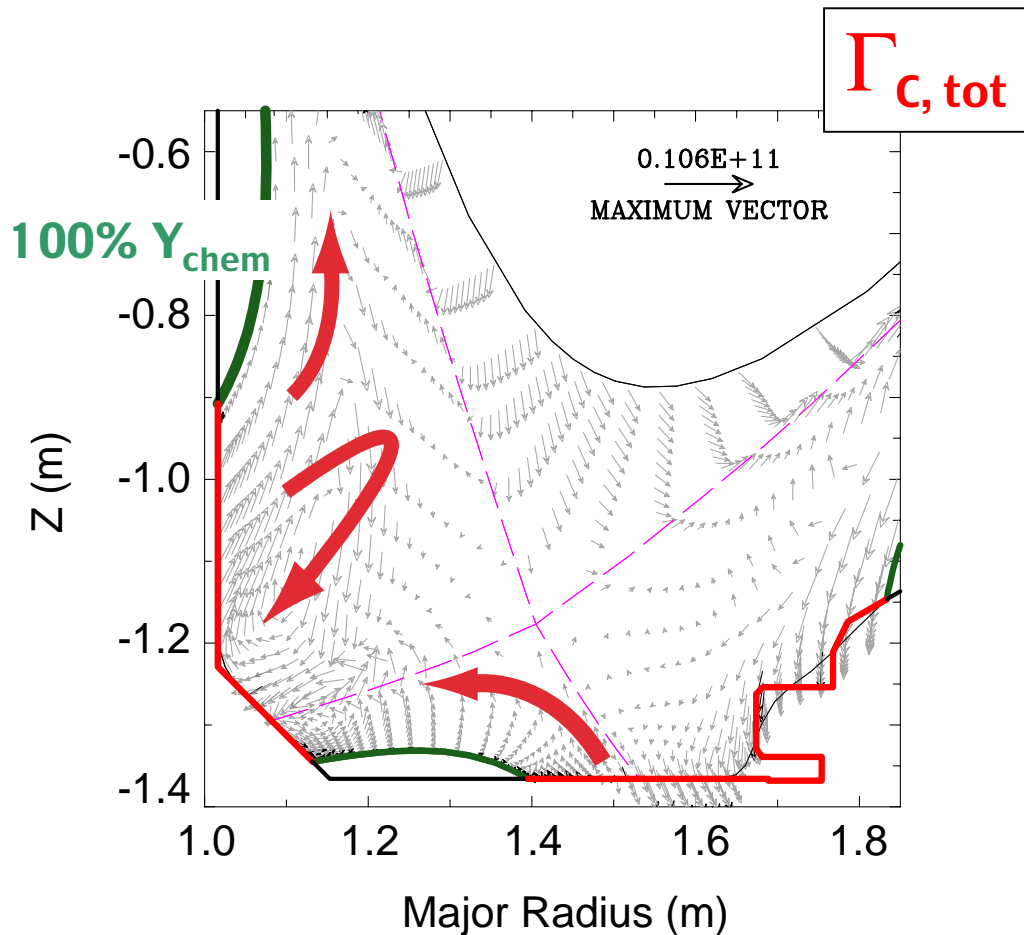


- MGe09:  $D_{\perp} = 0.65m^2/s$ ,  $\chi_e = \chi_i = 2.6m^2/s$ , MGe14:  $D_{\perp} = 0.38m^2/s$ ,  $\chi_e = \chi_i = 1.5m^2/s$

# Significant chemical sputtering of carbon on inner plate and divertor walls; outer plate region of net deposition



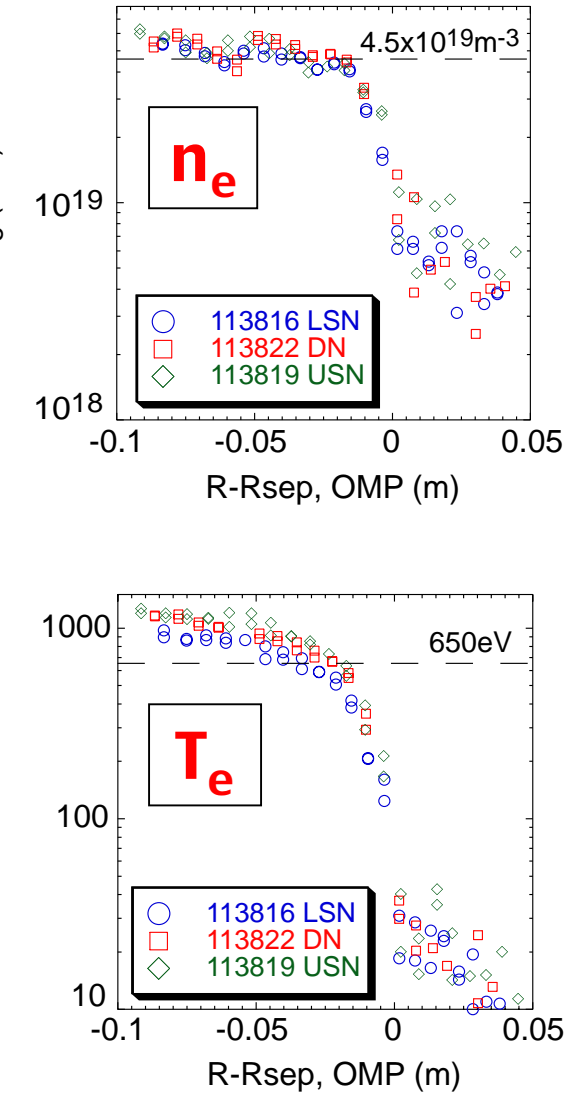
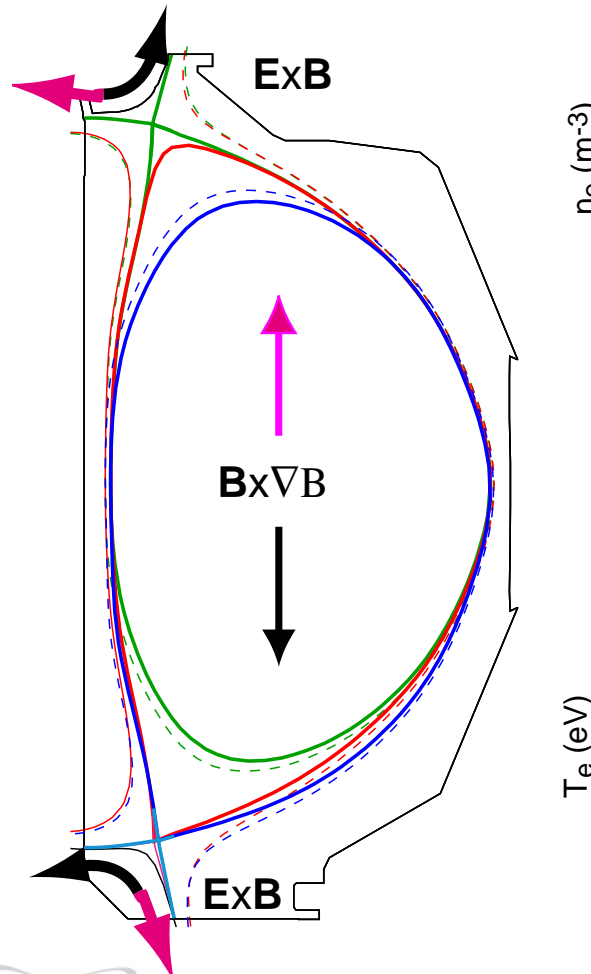
# UEDGE predicts ion carbon leakage into inner main SOL above the X-point due to dominant $\nabla T_i$ force



- Net transfer of carbon from outer to inner wall region
- Flow reversal away from inner target in far-SOL
- Leakage for  $Z > -0.8\text{m}$ :  $\nabla T_i$  force exceeds frictional drag from background plasma

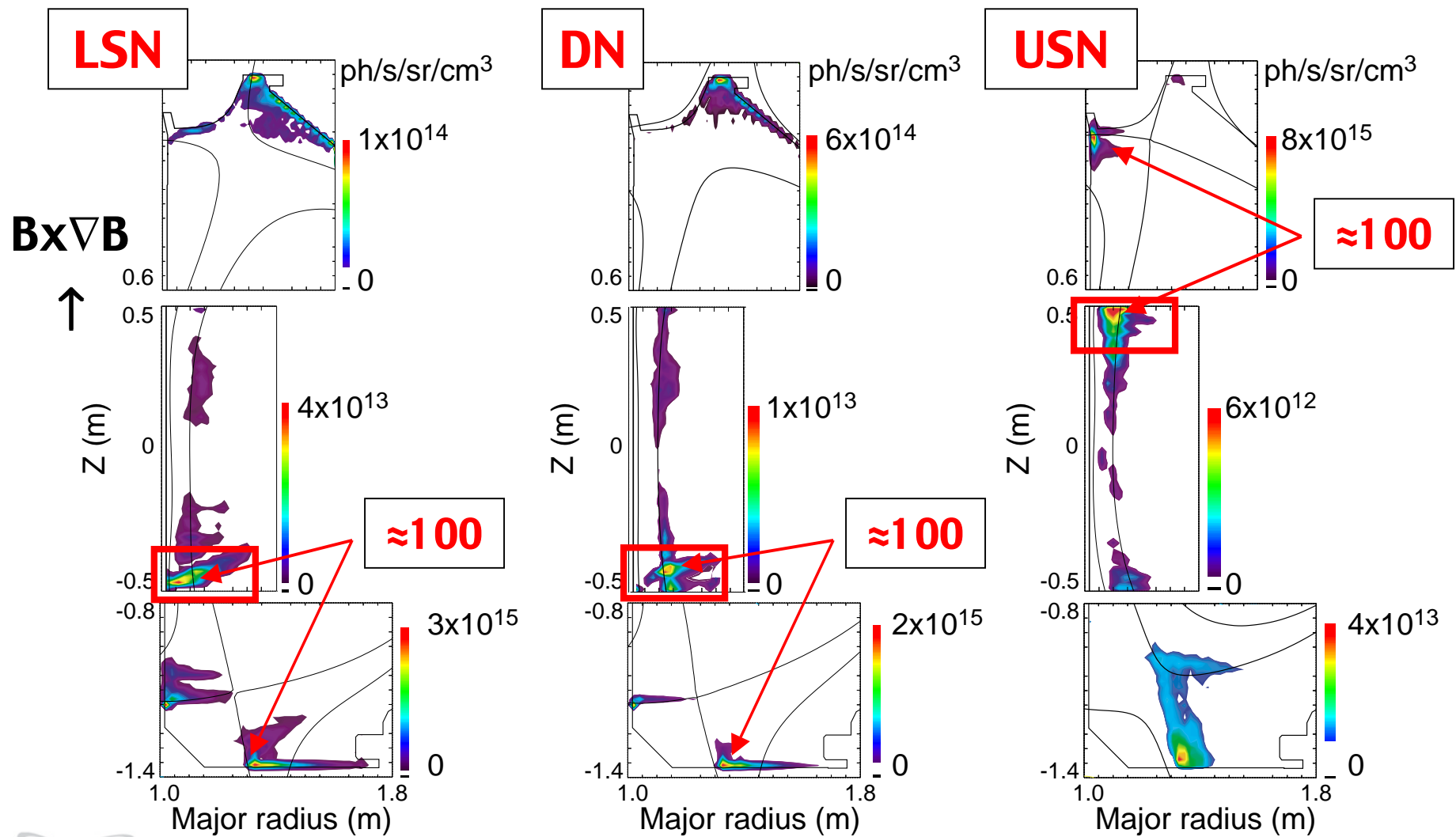
100%  $Y_{\text{chem}}$  + 100%  $Y_{\text{phys}}$

# Fueling and particle transport in medium-density ELMy H-mode in single and double-null configurations

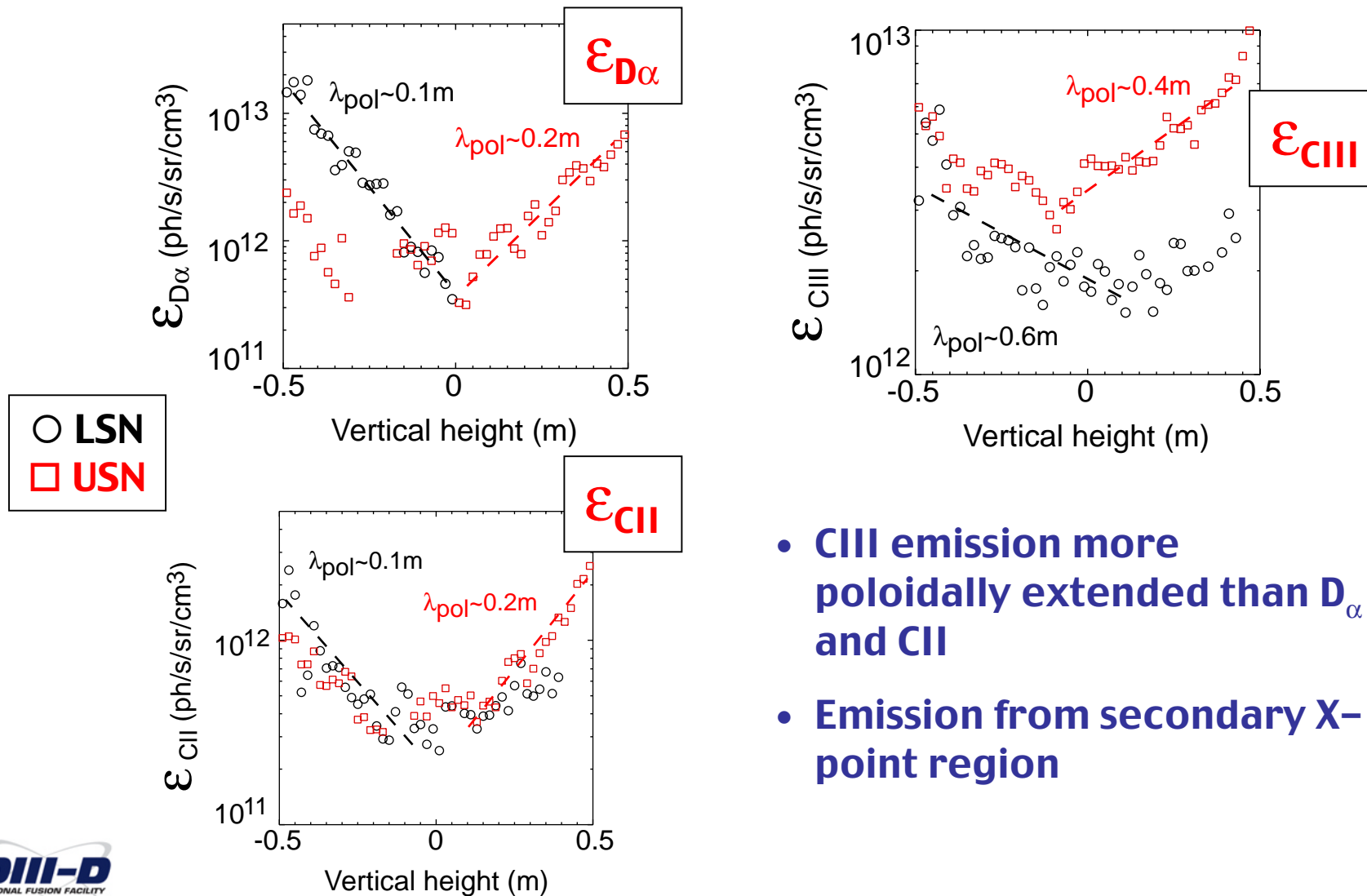


- Beam-heated ELMy H-modes:  $H_{89} \sim 2$
- $n/n_{GW} \sim 0.4$
- $dR_{\text{sep}} = 0, \pm 4 \text{ cm} < \text{outer gap} = 6 \text{ cm}$
- Vary direction of  $B_T$ , but keep  $I_p$ , to study effect of  $Bx\nabla B$  and  $ExB$

# $D_\alpha$ emission is strongest in primary divertor, in inner SOL it peaks nearest to primary X-point region



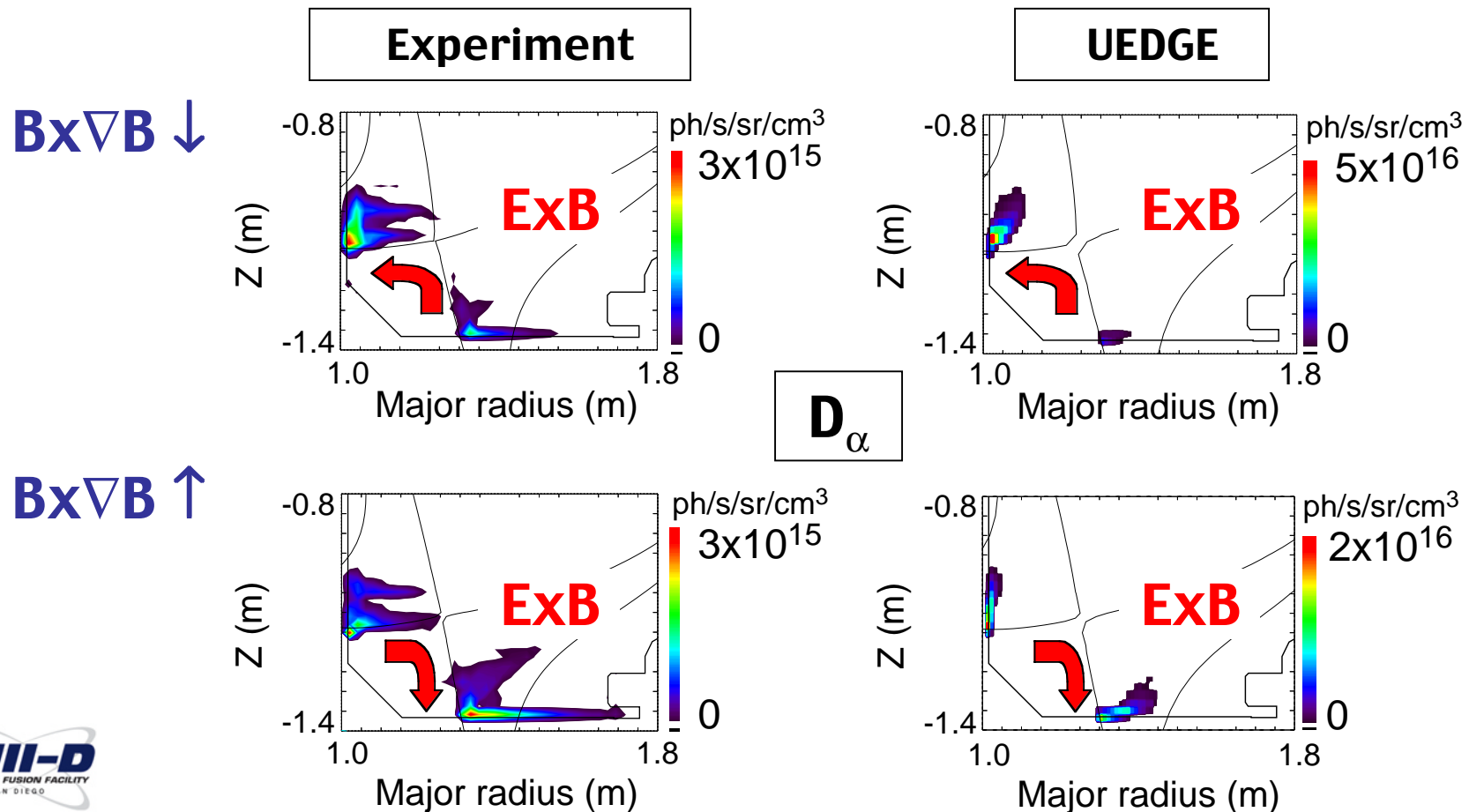
# Poloidal fall-off lengths of $D_\alpha$ , CII, CIII emission in inner midplane SOL only weakly dependent on divertor geometry and direction of ion $B_x \nabla B$



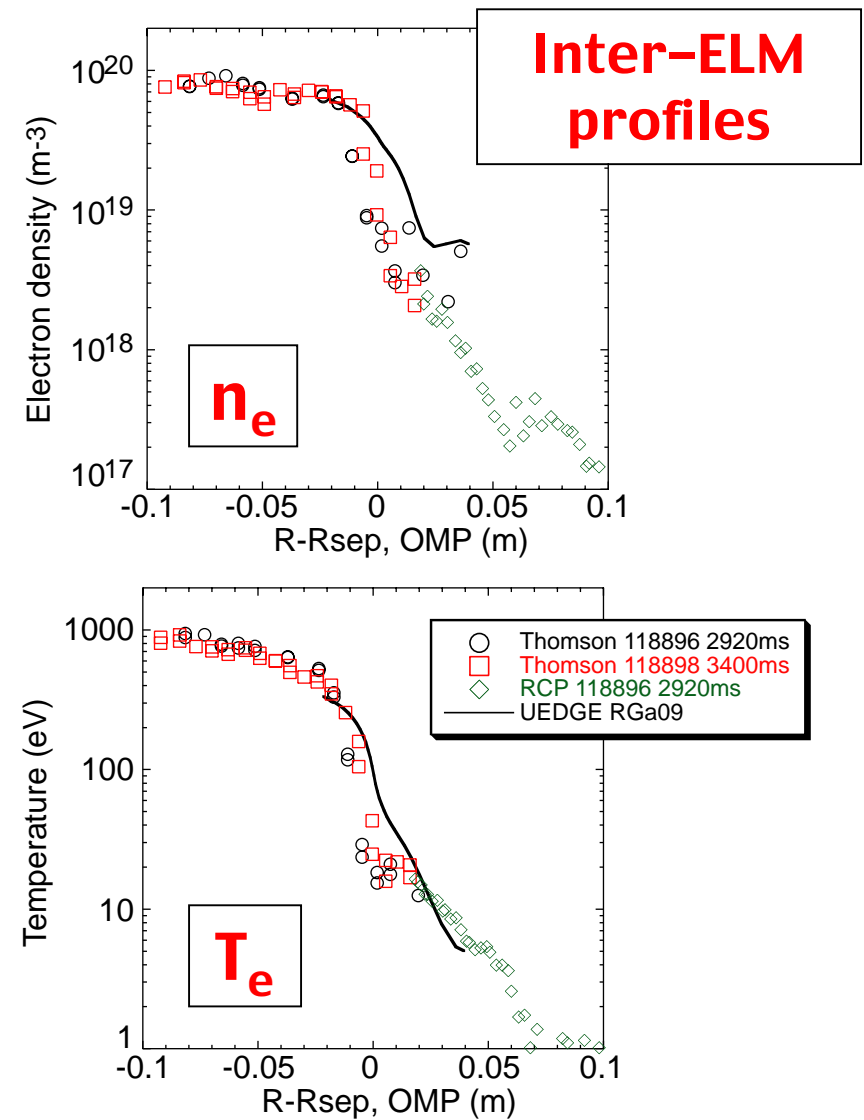
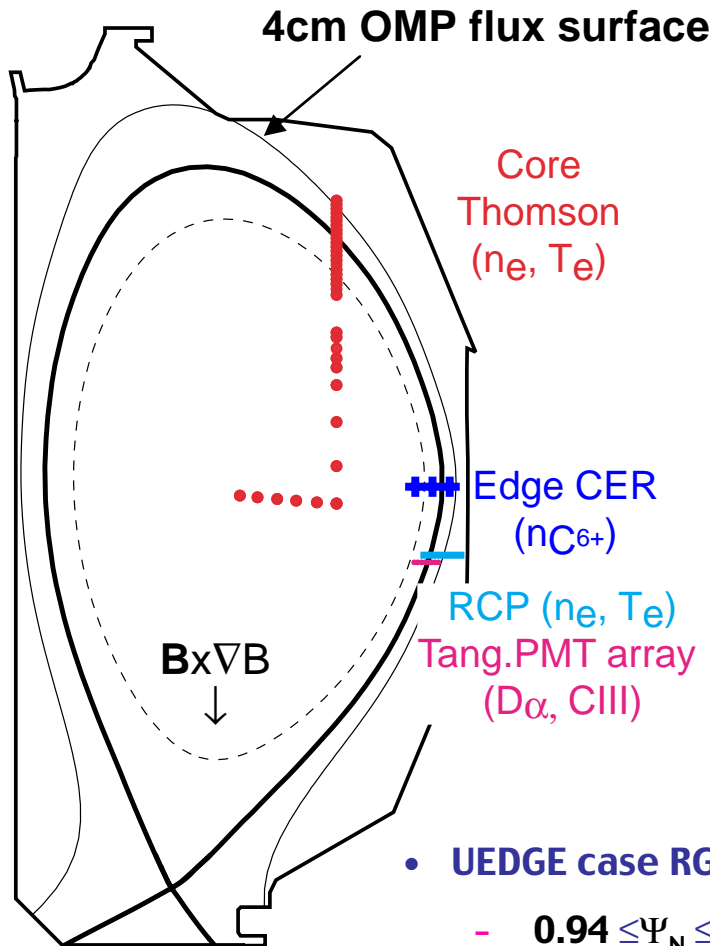
- CIII emission more poloidally extended than  $D_\alpha$  and CII
- Emission from secondary X-point region

# Effect of ExB drifts on $D_\alpha$ emission profiles stronger in the divertors than in inner midplane, qualitatively reproduced in UEDGE only when using drifts

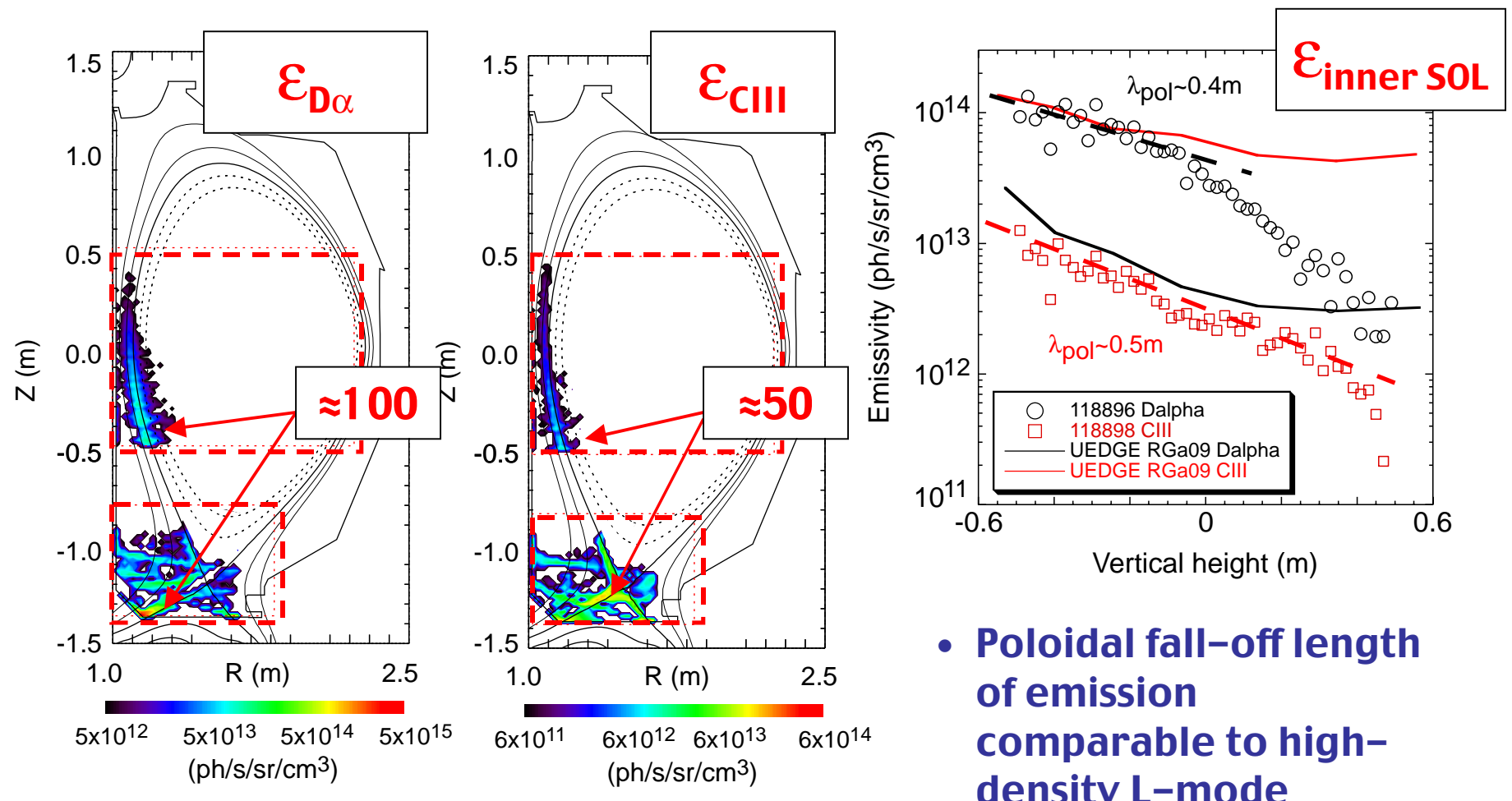
- Effects due to ExB drifts observed in both **upper and lower divertor**
- Modeling of inner midplane profiles shows variation with drift direction, not observed in the experiments



# Lower-single null ELMy H-mode with $n/n_{GW} = 0.7$ optimized for diagnosis of divertor and main SOL



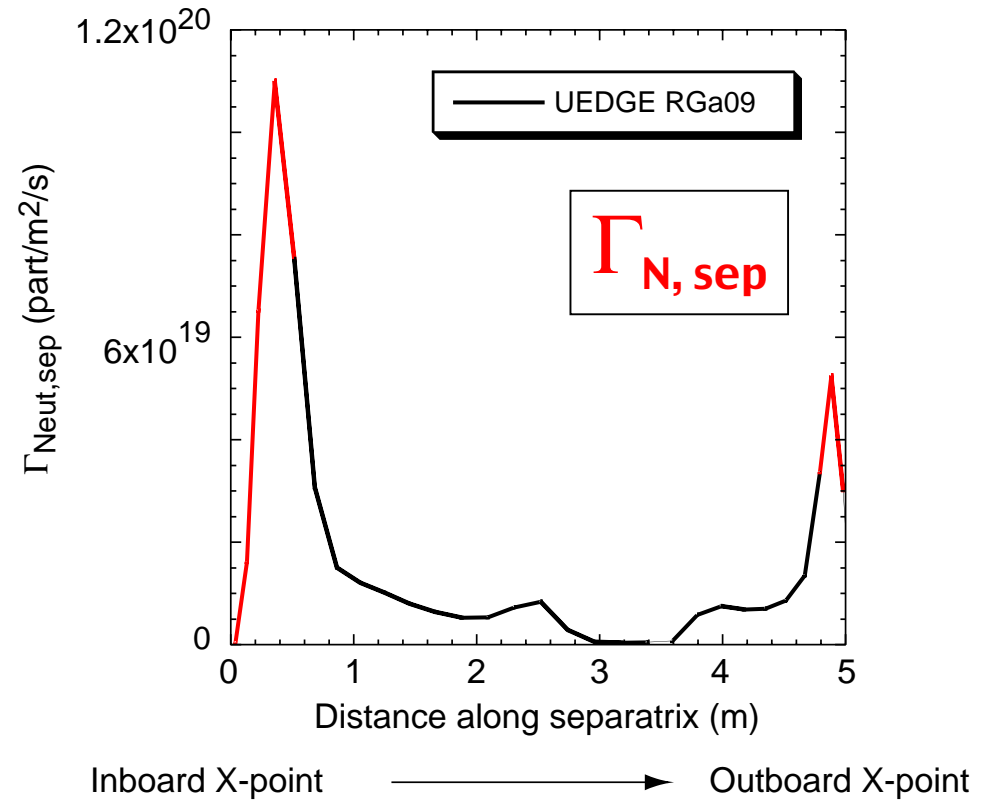
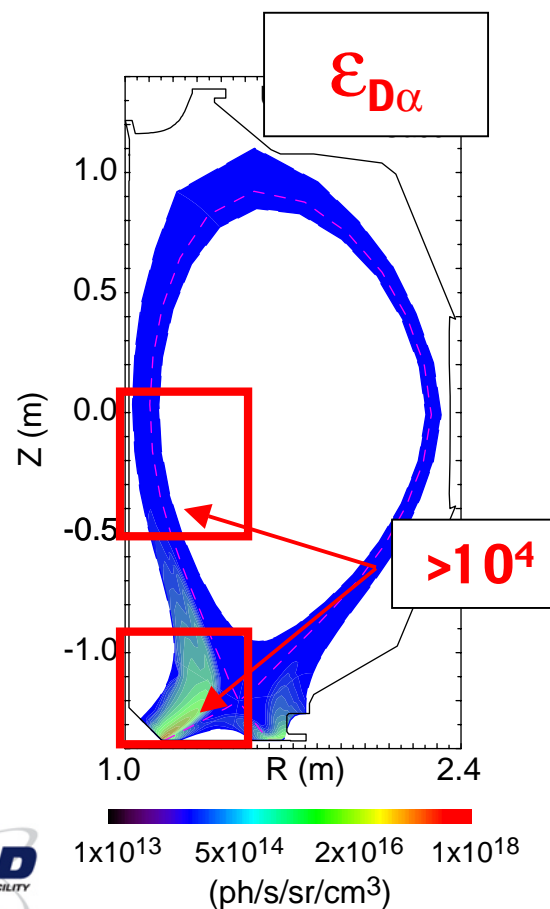
# Inner midplane $D_\alpha$ and CIII emission profiles strongly peaked toward lower divertor X-point



- Poloidal fall-off length of emission comparable to high-density L-mode

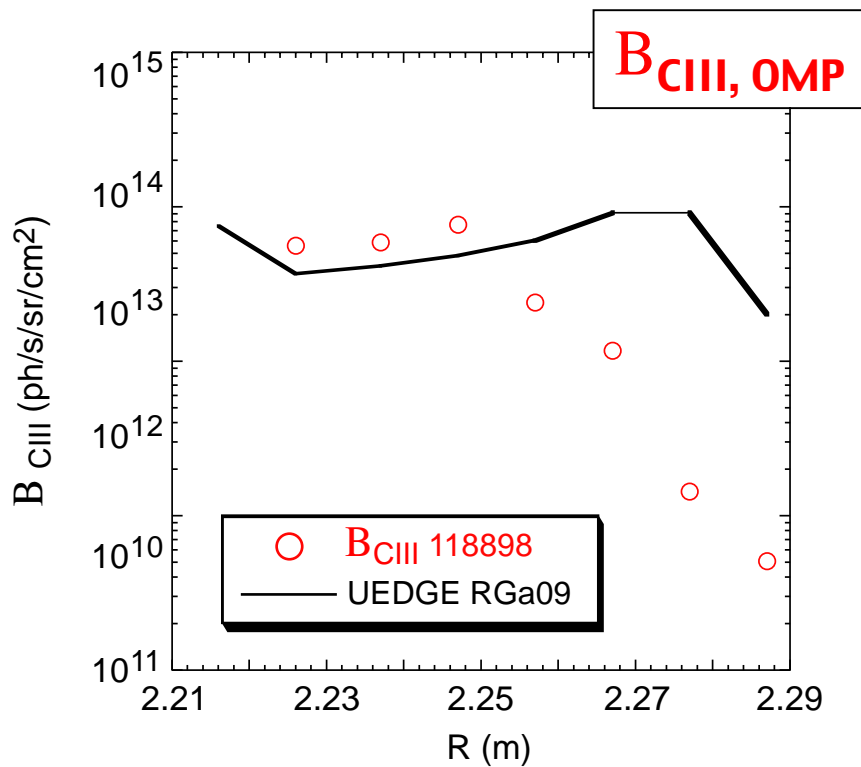
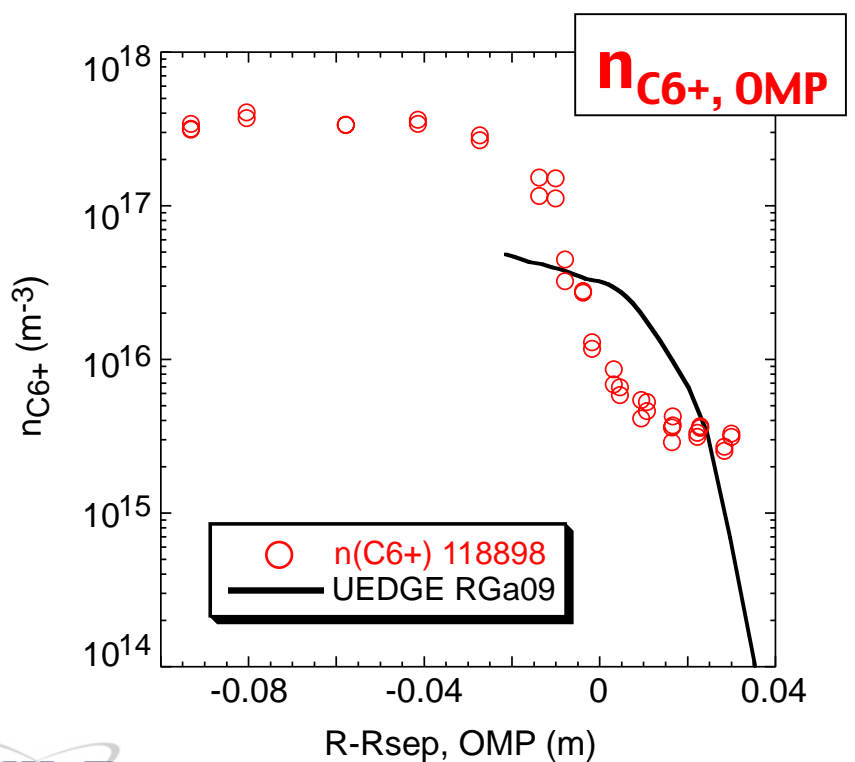
# Strong core plasma fueling from inner divertor and main SOL region calculated by UEDGE

- Significant neutral leakage from inner divertor region: divertor X-point fueling 63% of total core fueling, 37% neutral leakage → allowing leakage in halo region (DEGAS2) will increase this ratio

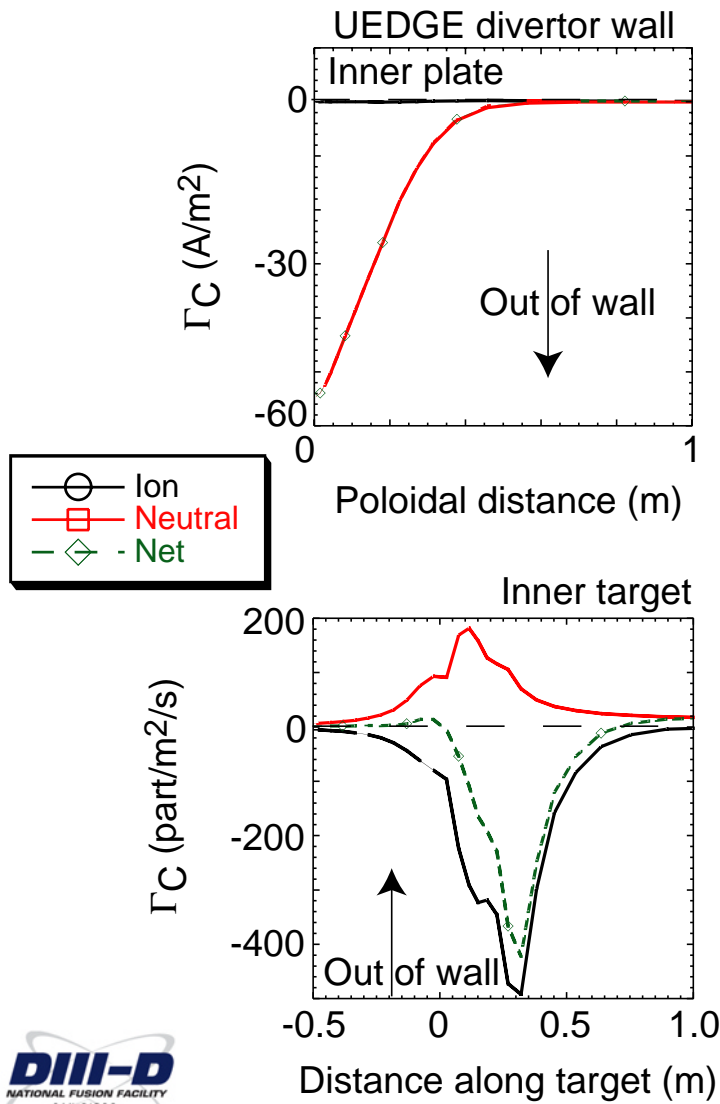


# Order-of-magnitude agreement between measured and calculated upstream carbon density and CIII emission

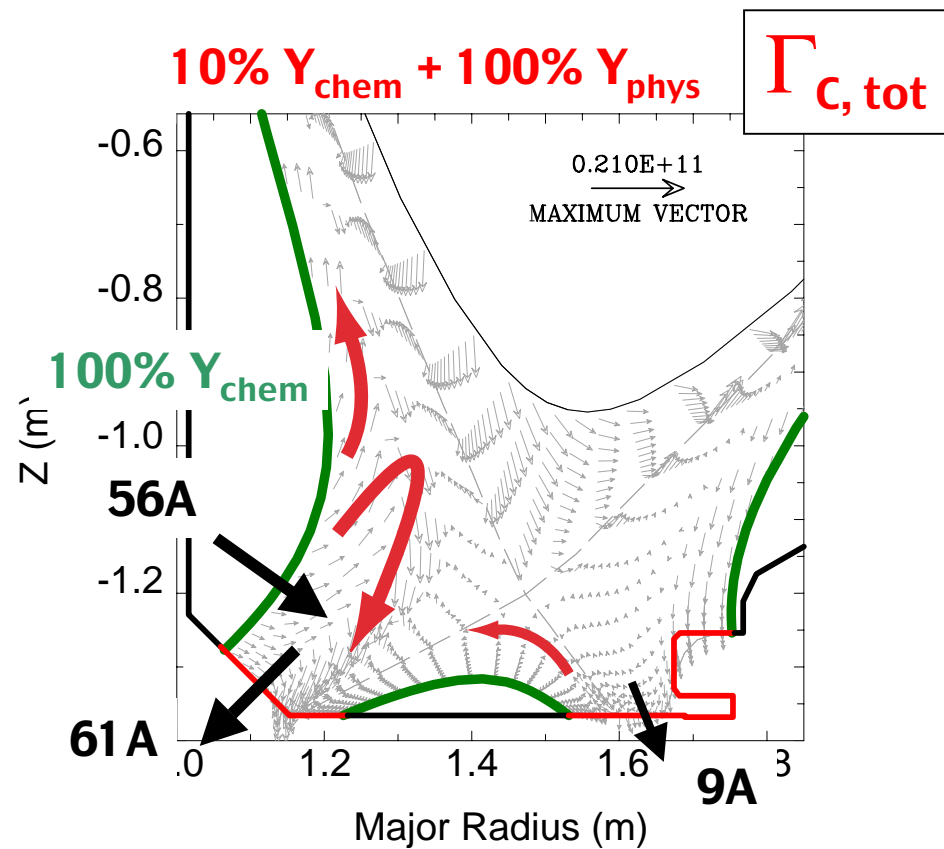
- Steep gradient region in UEDGE in SOL, measured inside separatrix
- Outer midplane CIII emission matched inside separatrix, but not in main SOL



# Main carbon source is inner divertor wall; inner and outer target plates are areas of net deposition



- Carbon leakage from inner divertor region due to flow reversal in far-SOL of inner divertor plasma



# Summary

---

- Assessment of poloidal distribution of core fueling in DIII-D L-mode and ELMy H-mode plasmas using ...
  - Detailed measurements of plasma parameters in the divertor and main SOL, including 2-D emission distribution of  $D_\alpha$ , CII, CIII
  - Data-constrained UEDGE/DEGAS2 2-D boundary modeling of deuterium neutrals and ions, and carbon transport
- Poloidal fueling distribution suggests that ...
  - Dominant core plasma fueling occurs near divertor X-point region due to recycling at the divertor targets
  - Significant neutral leakage from (colder) inner divertor into inner main SOL
- Divertor target plates and divertor walls are dominant carbon sources
- Carbon ion leakage from divertor into main SOL is the main transport mechanism that sets core carbon content